Microcontroller based Constant Voltage Battery Charger with Soft switching Buck Converter for Solar Home Lighting System

R.S.Sable[1], A.S.Werulkar[2] and P.S.Kulkarni[3]

Abstract— **This paper presents Design of a Microcontroller based Constant Voltage Battery Charger. The circuit is implemented using soft switching buck converter. Solar panels of 75Wp and 37WP are used in parallel for the experimentation and a lead acid battery of 75Ah is used for charging. Microcontroller Atmega16 is used for programming using Win AVR ISP software. It is observed that during 10AM to 2PM, on 1[st]may2012 when there is enough solar radiation at Nagpur, charging current of the battery is almost 7 to 8A.Time taken for charging the battery is 8 to 10 hours depending upon the intensity of solar radiation. The merits of the proposed charger are, highly efficient, simple to design mostly due to not having a transformer, puts minimal stress on the switch, and requires a relatively small output filter for low output ripple.**

***Index Terms*— Buck Converter, MOSFETs, Microcontroller.**

NOMENCLATURE

I : Output current in Amps.

Q : Carrier charge $1.6\times10^{-19}c$ in Coulombs.

V : Output voltage in Volts.

R_S : Series resistance in Ohm.

R_{sh} : Parallel resistance in Ohm.

I_{sc} : Short circuit current in Amps.

T_k : Absolute temperature in degree Kelvin.

n : Dielectric constant.

k : Boltzmann's constant $(1.38\times10^{-23}W\sec^0.k^{-1})$.

G_{ST} : Standard insolation in W/m$^{2.}$

T_{ST} : Standard temperature in degree Kelvin.

G : Environmental insolation in W/m$^{2.}$

[1]M.Tech student, Department of Electrical Engineering, Visvesvaraya National Institute of Technology, Nagpur , India; (e-mail:sable.rahul257@gmail.com)
[2] PhD Scholar, Department of Electrical Engineering, Visvesvaraya National Institute of Technology, Nagpur , India ; (e-mail:ashutoshwerulkar@gmail.com)
[3]Associate Professor, Department of Electrical Engineering, Visvesvaraya National Institute of Technology, Nagpur , India; (e-mail:pskulkarni@eee.vnit.ac.in)

V_{oc} : Open circuit voltage in Volt.

P_m : Peak Power in Watt.

I_L : Load current in Amps.

V_m : Maximum voltage in Volt.

I_m : Maximum current in Amps.

L_r : Resonant inductor in Henry.

C_r : Resonant capacitor in Farad.

L_0 : Low-pass filter in Henry.

Z_0 : Output impedance in Ohm.

W_0 : Angular frequency in rad/s.

f_r : Resonant frequency in Hz.

f_s : Switching frequency in Hz.

B_mT : Flux density.

J : Current density in A/m^2.

A_w : Window area mm^2.

A_c : Core area mm^2.

l_g : Length of air gap.

R_c : Core reluctance.

ZCS : Zero current switch.

η : Efficiency in $\%$.

I. INTRODUCTION

ENERGY is the basic requirement for the economic development of any country. Energy sector of Indian economy-agricultural, industry, transport, commercial, and domestic needs inputs of energy. The Ministry of New and Renewable Energy, Govt. of India has been implementing comprehensive programmes for the development and utilization of various renewable energy sources in the country. As a result of efforts made during the past quarter century, a number of technologies and devices have been developed and have become commercially available which includes biogas plants, solar water heaters, solar cookers, solar PV power plants, solar home lighting systems etc.[1]. To simplify the analysis, the output filter inductance is assumed to be sufficiently large to be considered as an ideal dc current source I_0 during a high-frequency resonant cycle [2,3].

In the literature many authors have proposed low cost and highly efficient design of DC-DC Buck/Boost converter. Nashed has suggested attractive advantages of PV technology which include a free and abundant fuel supply; little or no pollution or operation/maintenance costs (once installed), and unlimited system life[4]. Wai *et al*. have proposed to make the PV generation system more flexible and expandable, the backstage power circuit is composed of a high step-up converter and a pulse width-modulation (PWM) inverter. In the dc-dc power conversion, the high step-up converter is introduced to improve the conversion efficiency in conventional boost converters to allow the parallel operation of low-voltage PV arrays, and to decouple and simplify the control design of the PWM inverter [5]. Masheleni and Carelse explained Microcontroller based optimal battery chargers [6]. Siwakoti *et al*. have presented the Microcontroller Based Intelligent DC-DC Converter to track Maximum Power Point for Solar Photovoltaic Module [7]. X. Long *et al*. have proposed the development of battery-buffered photovoltaic (PV) power conditioning systems (PCSs) which is challenged by its cost/W. It compels the users to optimize the system's configuration in order to maximize the power generation. An alternative solution to this problem based on a charge collector (CC), which has the ability of maximizing the charge collection of battery is presented by the authors. The design of the CC is derived from the linear approximation model resolving prior probability distribution and dynamic DC/DC topology with microcontroller to meet the low-cost application. Low-cost charge collector of photovoltaic power conditioning system based dynamic DC/DC topology is explained in [8]. Ying-Chun Chuang has suggested zero-current switching (ZCS) operation to develop a novel soft-switching approach for rechargeable batteries. By inserting an auxiliary switch in series with a resonant capacitor, the proposed topology can obtain a novel ZCS buck dc–dc battery charger and significantly decrease the switching losses in active power switches. The proposed ZCS dc–dc battery charger has a straightforward structure, low cost, easy control, and high efficiency. The operating principles and design procedure of the proposed charger are thoroughly analysed [9]. Ying-Chun Chuang and Yu-Lung Ke presented a novel High-Efficiency Battery Charger with a Buck Zero-Voltage-Switching Resonant Converter [10]. Swapnajit Pattnaik *et al*. have proposed the Efficiency Improvement of Synchronous Buck Converter by Passive Auxiliary Circuit [11]. Divakar and Danny Sutanto presented Optimum Buck Converter with a Single Switch [12].

This paper proposes a soft switching buck converter using microcontroller ATMEGA 16. In this buck converter, a

Main switch auxiliary switch has been used with main inductor and capacitor as well as resonant inductor and capacitor. Voltage from solar panel has been decreased to 14V in buck mode. This buck converter may be used to fully charge the lead acid battery. Using microcontroller improvement is continuously possible by changing the logic in the program and PWM adjustment is easy to track maximum power point on the solar panel. It has a significant impact on the efficiency of the system.

II. CHARACTERISTICS OF SOLAR CELL AND MODULE

Various parameters of a solar module:

Fig.1 shows the equivalent Circuit of a Solar Cell. Equations (1)-(3) describe the behavior of a Solar Cell in mathematical form.

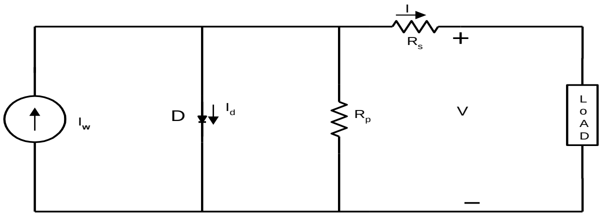

Fig.1. Equivalent circuit of a solar Module.

The Current-Voltage relationship of a solar PV module is given by the following equations and Fig.2 shows the I-V characteristics of the 37 W_p solar panel with different solar radiation.

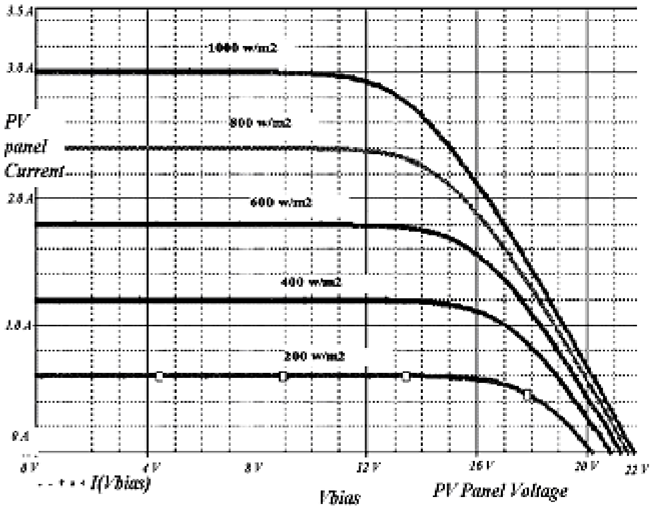

Fig.2. Simulated I-V characteristics of 37Wp solar panel.

$$I = I_{SC} - I_0 \left\{ \exp\left[\frac{q(V + R_S I)}{nKT_K} \right] - 1 \right\} - \frac{V + R_S I}{R_{th}} \quad (1)$$

$$\Delta I = \alpha_{SC-T} \left(\frac{G}{G_{ST}} \right) * (T_{ST} - T) + \left(\frac{G}{G_{ST}} - 1 \right) * I_{SC-ST} \quad (2)$$

$$\Delta V = -\beta_{OC-T} * (T_{ST} - T) - R_S * \Delta I \quad (3)$$

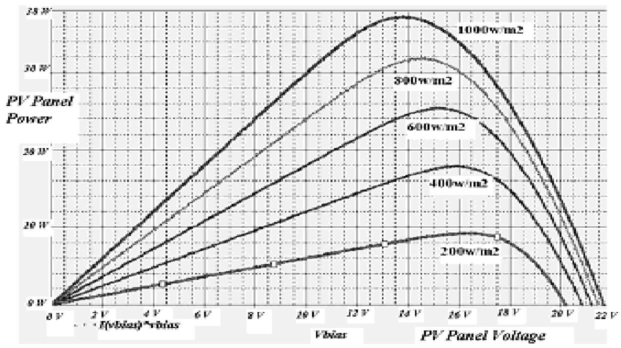

.

Fig.3. Simulated P-V characteristics of 37Wp solar panel.

Fig.3. shows Simulation of Power versus curve for varying solar Radiation with 37 watt panel.

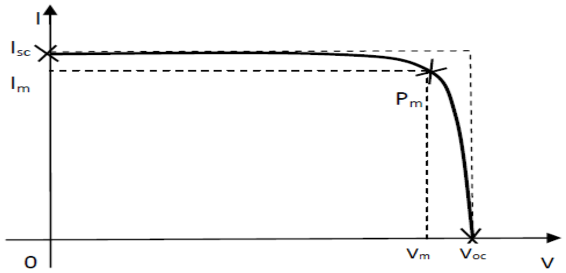

Fig4. Current-voltage (I-V) curve of a solar PV module.

Corresponds under and standard Test condition (STC) to ($AM1.5$, $1000W/m^2$ and $25°C$ cell temperature of a PV module). Under the STC the power output of a PV module is maximum; therefore it is also referred as peak power or Watt (peak) or W_P. This is given as product of V_m and I_m (Refer Fig .4)

$$V_{oc} = \frac{KT}{q} \ln\left(\frac{I_L}{I_0} + 1\right) \quad (4)$$

$$P_m = V_m \times I_m \quad (5)$$

Fill Factor:

$$FF = \frac{V_{oc} - \ln(V_{oc} + 0.72)}{V_{oc} + 1} \quad (7)$$

The Fill Factor (FF) of a PV module is actually the area under the *I-V* curve. It is given in percentage.

$$FF = \frac{V_m I_m}{V_{oc} I_{sc}} \% \quad (8)$$

Efficiency:

The module efficiency is written as:

$$\eta = \frac{P_{max}}{P_{in}} = \frac{V_m I_m}{P_{in}} = \frac{V_{oc} I_{sc} FF}{P_{in}} \% \quad (9)$$

III. DESIGN OF SOFT SWITCHING BUCK CONVERTER TYPE BATTERY CHARGER FOR SOLAR HOME LIGHTING SYSTEM.

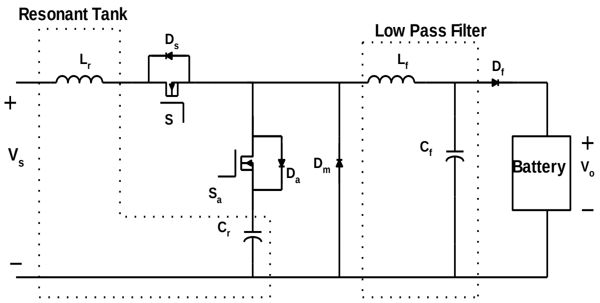

Fig.5. ZCS buck converter for battery charger.

The ZCS buck converter has an additional *LC* resonant tank. It generates zero-current condition for the device to turn off. Unlike traditional buck converters, this ZCS buck resonant converter has an extra resonant tank. It consists of a resonant inductor L_r, a resonant capacitor C_r, and a diode D_m. The inductor L_r is connected in series to a power switch S to limit the di/dt of the power switch S, and capacitor C_r is an auxiliary energy transfer element. The diode D_m is a freewheeling diode. The capacitor C_f and inductor L_f *are* low-pass filters, for filtering high-frequency ripple signals and providing a stable dc source for battery charging. The switching signals required for main switch and auxiliary switch are generated from PWM port pin of microcontroller Atmega16.

a. Operation Principle

To simplify the analysis, the output filter inductance is assumed to be sufficiently large to be considered as an ideal dc current source I_0 during a high-frequency resonant cycle.

Before analyzing the operation modes of the presented circuit, the circuit parameters are defined as follows:

1) Characteristic impedance $Z_0 = \left(\frac{L_r}{C_r}\right)^{1/2}$ (10)

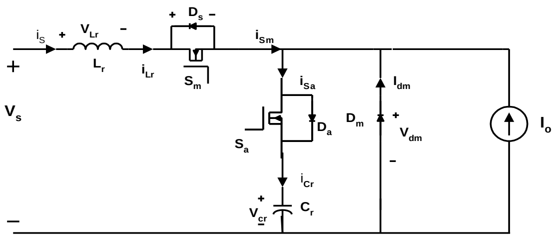

Fig.6. Equivalent circuit of novel ZCS buck converter for battery charger.

2) Resonant angular frequency $\omega_0 = \frac{1}{(L_r/C_r)^{1/2}}$ (11)

3) Resonant frequency $f_r = \frac{\omega_0}{2\pi}$ (12)

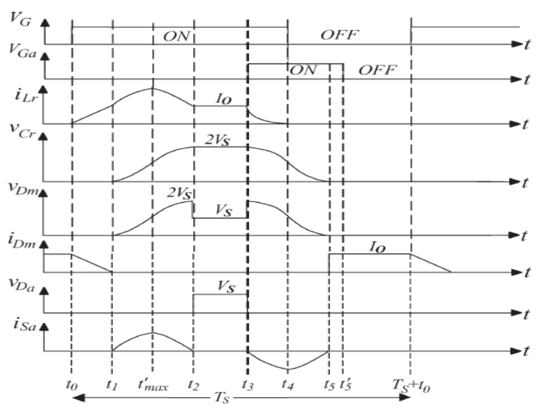

Fig.7. Key waveforms of the proposed novel charger.

b. Design of Buck Converter for Solar Home Lighting System

Assume Input Voltage from Solar Panel at MPP=$17.5V$

Output voltage required for battery charging= $14V$

Assume Switching Frequency, $f_s = 20kH_z$

Capacity of present PV modules Solar Panel= $37W_p + 75W_p = 112W_p$

Maximum Charging Current= $112/12 = 10A$.

Taking higher value, Maximum Output Current= $15A$

The equivalent output impedance= $V_0/I_0 = \frac{14}{15} = 1\Omega$,

$Q = 1$ (13)

Hence characteristic Impedance, $Z_0 = \frac{R_0}{Q} = 1\Omega$ Assume

$$f_{ns} = 0.7 \quad (14)$$

The necessary resonant frequency is derived from

$$f_0 = \frac{f_s}{f_{ns}} = \frac{20kHz}{0.7} = 28.57kHz \quad (15)$$

Resonant Angular Frequency,

$$w_0 = (L_r x C_r)^{-1/2} \quad (16)$$

$$= 2\pi \times f_0 = 179.51 \times 10^3 rad/s \quad (17)$$

$$L_r = Z_0/\omega_0 = \frac{1}{179.51 \times 10^3 rad/s} = 5.57\mu H \quad (18)$$

$$C_r = \frac{1}{\omega_0 \times Z_0} = \frac{1}{179.51 \times 10^3 rad/s} = 5.57\mu F \quad (19)$$

To limit charging current ripple and the output voltage ripple, the circuit parameters for the low pass filter of the ZCS battery charger are set as follows.

$$L_0 = 100L_r = 100 \times 5.57 = 557\mu H . \quad (20)$$

$$C_0 = 100C_r = 100 \times 5.57 = 557\mu F . \quad (21)$$

TABLE I
CIRCUIT PARAMETERS

Solar panel	$37+75=112W_p$
Input Voltage V_s	17.5 V
Switch Frequency fs	20 kHz
Resonant Frequency fo	28.57kHz
Output voltage Vo	14 V
Resonant inductor L_r	5.57 µH
Resonant Capacitor	5.57µF
Filter Inductor Lo	557 µH
Filter Capacitor	557 µF
Main switch	IRFZ44N
Auxiliary switch	IRFZ44N

IV. DESIGN PROCEDURE OF RESONANT INDUCTOR AND CAPACITOR

The inductor consists of a magnetic circuit and an electrical circuit. The design requires i)the size of wire to be used for the electric circuit to carry the rated current safely, ii) the size and shape of magnetic core to be used such that the peak flux is carried safely by the core without saturation. The required sizes of the conductors are safely accommodated in the core and iii) the number of turns of the electric circuit to obtain the desired inductance.

$$A_c A_w = \frac{LI_p I_{max}}{K_w B_m J} = \frac{5.57 \times 10^{-6} \times \sqrt{2} \times 15 \times 15}{0.3 \times 0.2 \times 3 \times 10^6 A/m^2} = 9.8 \times 10^3 mm^4 \quad (22)$$

$$A_c = 1.36 \times 100mm^2 \; A_w = 0.747 \times 100mm^2 \quad (23)$$

$$N = \frac{LI_p}{B_m A_c} = \frac{5.57 \times 10^{-6} \times \sqrt{2} \times 15}{0.2 \times 1.36 \times 100} = 4.34 \text{ Turn} \quad (24)$$

Selecting the $N = 5$.

V. SIMULATION RESULTS

Fig.8 shows the simulation diagram of soft switching buck converter. In this buck converter has been designed using main switch and auxiliary switch.

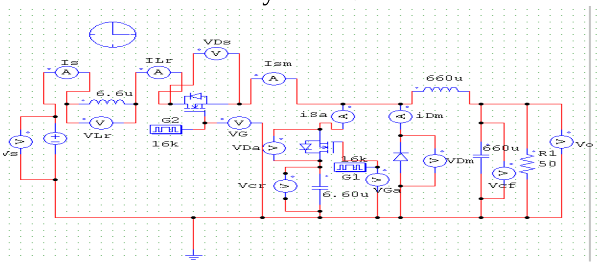

Fig.8. Simulation Diagram on Psim Simulation software for Soft switching Buck Converter.

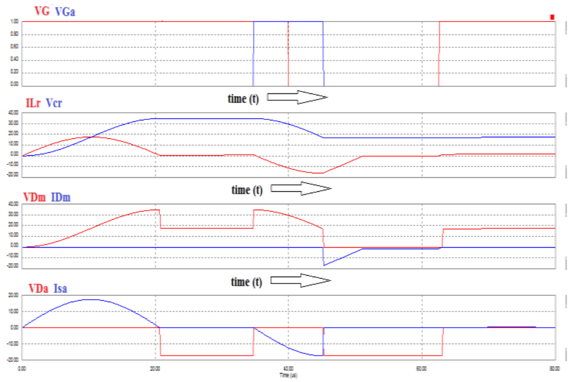

Fig.9 Simulation Waveform on Psim Simulation software for Soft switching Buck Converter.

Fig.9. shows the simulation waveform of soft switching buck converter. Gate pulse across the auxiliary switch and main switch, current across the inductor is shown in Fig.9 with red waveform and blue is for voltage across the capacitor. Diode voltage is in red waveform and current is in blue.

VI. EXPERIMENTAL HARDWARE RESULTS

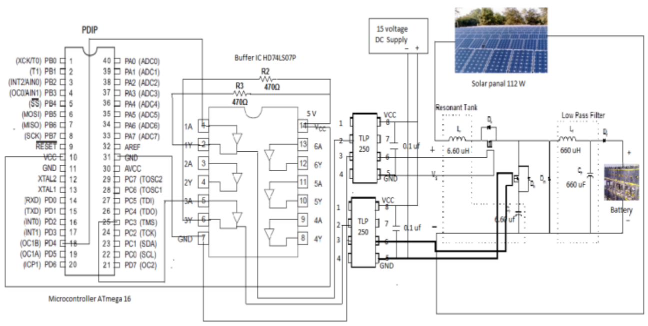

Fig.10 connection diagram of buck converter.

Fig.10. shows the connection diagram of buck converter. PWM gate pulse is generated by the microcontroller AT

mega 16. This pulse before applying to the gate pulse of MOSFET IRFZ44N will pass through gate driver circuit and Buffer IC 7407 is for the protection of microcontroller.

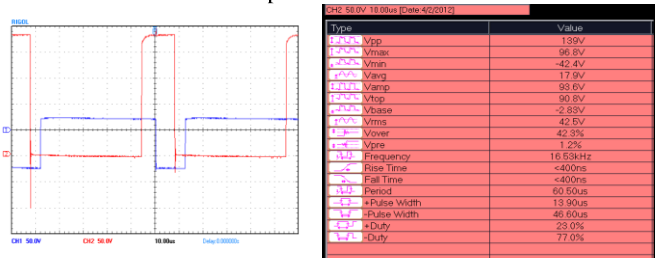

Fig.11 Gate pulse VG & VGa Result in Hardware**.**

Fig. 11 shows hardware result of gate pulse where normal waveform is for the main switch and delayed waveform is for the auxiliary switch.

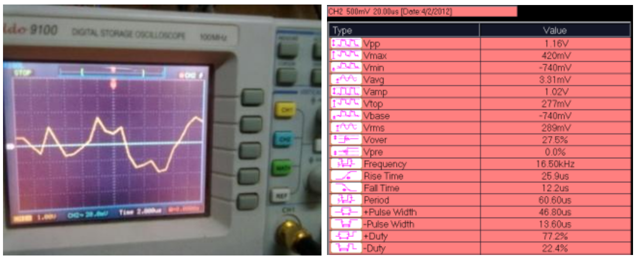

Fig. 12 Voltage Waveform across the diode VDm

Fig.12. shows the Hardware result of Voltage waveform across the diode.

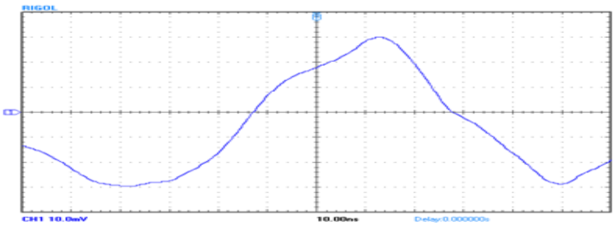

Fig.13Current Waveform across the source Isa.

Fig.13.shows the hardware result of current waveform passing through source Isa.

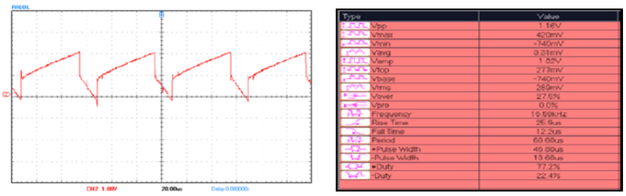

Fig.14 Voltage waveform across the capacitor.

Fig.14. shows the hardware result of Voltage waveform across the capacitor V_{cr}.

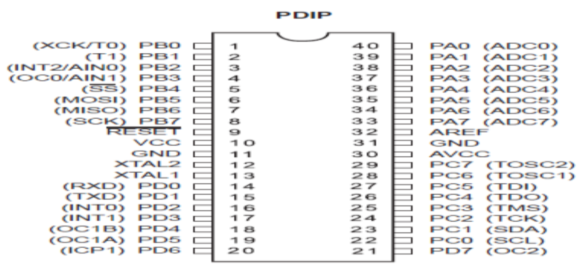

Fig.15 Pin Configuration ATmega16.

Fig.15. shows the pin configuration of ATmega16.The ATmega16 is a low-power CMOS 8-bit microcontroller based on the AVR enhanced RISC architecture. By executing powerful instructions in a single clock cycle, the ATmega16 achieves throughputs approaching 1 MIPS per MHz allowing the system design to optimize power consumption versus processing speed. The AVR core combines a rich instruction set with 32 general purpose working registers. All the 32 registers are directly connected to the Arithmetic Logic Unit (ALU), allowing two independent registers to be accessed in one single instruction executed in one clock cycle.

This paper shows the experimental results of the PWM waveform generated through Microcontroller. This microcontroller is used for generating the Gate signal to the MOSFET switch IRFZ44N of the soft switching converter. The work also shows the simulated output of the Soft switching buck converter. For generating Closed loop PWM, Microcontroller Atmega16 is used. This Microcontroller will generate the PWM in such a way that it will try to work at maximum power point. The DC - DC converter may work in Boost or Buck mode as per the requirement of the load and the battery.

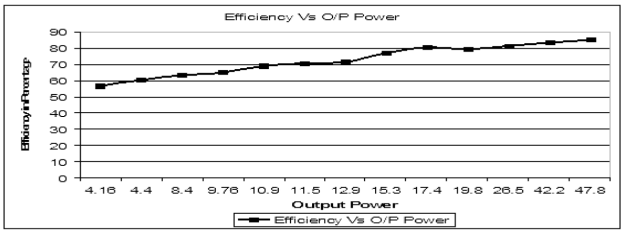

Fig.16 Efficiency Vs. Output Power.

Fig.16. shows Efficiency Vs. output Power. The graph shows that the efficiency increases with increase in output power.

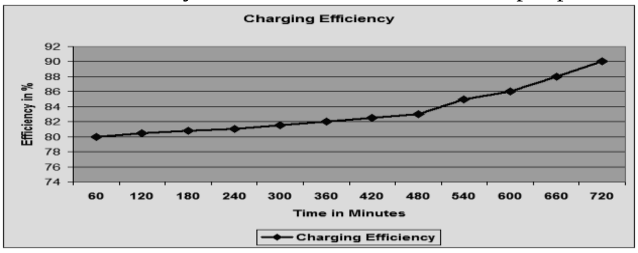

Fig.17 Charging efficiency of the 75Ah battery.

Fig.17. shows A rheostat of 100Ω / $5A$ rating was used to note the output power.

Fig.18 Final Photograph of the developed circuit

Fig.18. shows the development board of microcontroller and buck converter with gate driver final PCB .

Fig.19 Experimental Arrangement

Fig.19. shows the experimental arrangement of buck converter.

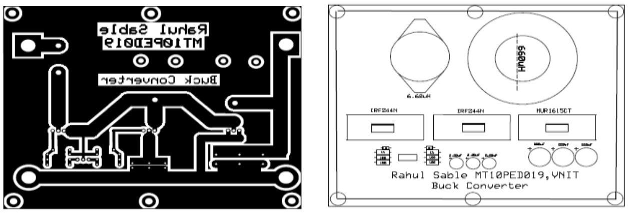

Fig.20.(a) PCB layout of bottom layer buck converter Fig.20.(b) PCB layout silk screen of buck converter.

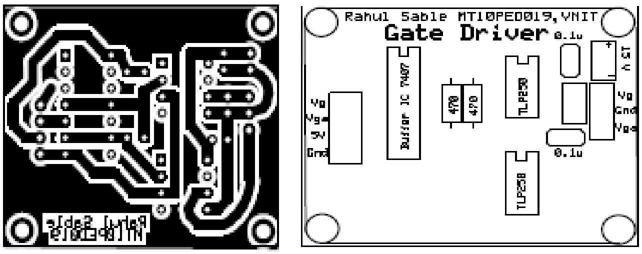

Fig.21. (a) PCB layout of bottom layer Gate driver. Fig.21. (b) PCB layout of silk screen of Gate driver.

The PCB layout is made in Express PCB software Buck converter circuit and Gate driver is shown in Fig.20 & Fig. 21 respectively .Fig.20 (a) is for bottom layer and Fig.20 (b) is for silk screen of buck converter.Fig.21.(a) is for bottom layer andFig.21.(b)is for silk screen of Gate driver.

VII. CONCLUSION

The Software simulated output of the buck converter is generated using MULTISIM software. The hardware results are shown using Caddo9100 series DSO $100MHz$. Fig.6 and Fig. 9 show the completed theme, the experimental and simulated results of the executed part of the project resepctively. **By using the soft switching technique, the switching losses were minimized as compared to the hard switching technique. In the hard switching technique, generally the efficiency which is less, is improved and reached to around 90 % by using ZVS soft switching technique.The efficiency of the converter changes from 75% to 89 % for load variation from 3W to 36 W.** The Solar charge controller is being designed using dynamic buck boost converter topology. In this topology, it is being ensured that PWM generation through microcontroller ATmega16 will be controlled depending upon solar radiation intensity and temperature.

ACKNOWLEDGMENT

The authors thank the authorities of VNIT, Nagpur and SVPCET, Nagpur for providing facilities to carry out the research work.

REFERENCES

[1] C.S. Solanki :*Solar Photovoltaics: Fundamentals, Technologies and Applications,* PHI Learning Private Limited, New Delhi, India 2009.

[2] V. Ramanarayanan "*Course Material on Switched Mode Power Conversion*" September 12, 2005.

[3] N.Mohan , Tore M. Undeland and William P. Robbings", *Power electronics converters , application,and Design*" Second Edition. 1995.

[4] M.N.F.Nashed, "Low Cost Highly efficient of complete PV System*", IEEE Transactions on Energy Conversion, Vol. 3, No. 3, pp. 503-506 ,September 1988.*

[5] R.J. Wai, W. H. Wang and C.Y. Lin, "High- Performance Stand Alone Photovoltaic Generation Syetem", *IEEE Transaction of Industrial Electronics, vol.55,No..pp.240-25, 1 January 2008.*

[6] H.Masheleni and X.F. Carelse, "Microcontroller-Based Charge Controller For Stand-Alone Photovoltaic System", *Solar Energy,Vol.61,No.4,pp. 225-230,1997.*

[7] Siwakoti, Y.Prasad, Bhupendra Bimal Chhetri, Brijesh Adhikary and Diwakar Bista, "Microcontroller Based Intelligent DC-DC Converter to Track Maximum Power Point For Solar Photvoltaic Module*", IEEE conference pp.(94-101),2010.*

[8] X. Long,R. Liao and J. Zhou1 "Low-cost charge collector of photovoltaic power conditioning system based dynamic DC/DC topology" *IET Renew, Vol. 5, Iss. 2, pp. 167–174, Power Gener., 2011.*

[9] Y.Chun Chuang, "High-Efficiency ZCS Buck Converter for Rechargeable Batteries", *IEEE Transaction of Industrial Electronics, Vol. 57, NO. 7, JULY 2010.*

[10] Y. Chuang and Y.Lung Ke, Senior Member, "A Novel High-Efficiency Battery Charger With a Buck Zero-Voltage-Switching Resonant Converter" *IEEE Transaction on Energy Conversion,Vol.22, NO. 4, December 2007.*

[11] S. Pattnaik, A. K. Panda, and K. Mahapatra "Efficiency Improvement of Synchronous Buck Converter by Passive Auxiliary Circuit" *IEEE* Transaction on Industrial *Applications, VOL. 46, NO. 6,November/ December 2010.*

[12] B. P. Divakar and Danny Sutanto" Optimum Buck Converter with a Single Switch" *IEEE* Transaction *on power Electronics VOL.14,NO.4,JULY1999.*

[13] Rahul S. Sable, A. S. Werulkar and P. S. Kulkarni , "Microcontroller Based Soft Switching Buck Converter for Solar Home Lighting System*.",Proceeding of National Conference on Emerging Technologies in Renewable Energy & Elecrtical Engineering (ETREEE-2012)ITM Bhilwara (Rajesthan) pp.(167-173), February 25-26,2012.*